Available online at www.sciencedirect.com
SCIENCE DIRECT
Biochimica et Biophysica Acta 1749 (2005) 103–112
BIOCHIMICA ET BIOPHYSICA ACTA
BBA
http://www.elsevier.com/locate/bba

Two consecutive aspartic acid residues conferring herbicide resistance in tobacco acetohydroxy acid synthase

Dung Tien Le[a,1], Moon-Young Yoon[b], Young Tae Kim[c], Jung-Do Choi[a,*]

[a]School of Life Sciences, Chungbuk National University, Cheongju 361-763, South Korea
[b]Department of Chemistry, Hanyang University, Seoul 133-791, South Korea
[c]Department of Microbiology, Pukyong National University, Busan 608-737, South Korea

Received 14 December 2004; received in revised form 22 February 2005; accepted 24 February 2005
Available online 11 March 2005

Abstract

Acetohydroxy acid synthase (AHAS) catalyzes the first common step in the biosynthesis pathway of the branch chain amino acids in plants and microorganisms. A great deal of interest has been focused on AHAS since it was identified as the target of several classes of potent herbicides. In an effort to produce a mutant usable in the development of an herbicide-resistant transgenic plant, two consecutive aspartic acid residues, which are very likely positioned next to the enzyme-bound herbicide sulfonylurea as the homologous residues in AHAS from yeast, were selected for this study. Four single-point mutants and two double mutants were constructed, and designated D374A, D374E, D375A, D375E, D374A/D375A, and D374E/D375E. All mutants were active, but the D374A mutant exhibited substrate inhibition at high concentrations. The D374E mutant also evidenced a profound reduction with regard to catalytic efficiency. The mutation of D375A increased the K_m value for pyruvate nearly 10-fold. In contrast, the D375E mutant reduced this value by more than 3-fold. The double mutants exhibited synergistic reduction in catalytic efficiencies. All mutants constructed in this study proved to be strongly resistant to the herbicide sulfonylurea Londax. The double mutants and the mutants with the D375 residue were also strongly cross-resistant to the herbicide triazolopyrimidine TP. However, only the D374A mutant proved to be strongly resistant to imidazolinone Cadre. The data presented here indicate that the two residues, D374 and D375, are located at a common binding site for the herbicides sulfonylurea and triazolopyrimidine. D375E may be a valuable mutant for the development of herbicide-resistant transgenic plants.

Keywords: Acetohydroxy acid synthase; Conserved aspartic acid; Herbicide resistance; Tobacco; Site-directed mutagenesis

1. Introduction

In most organisms in which acetohydroxy acid synthase (AHAS, EC 2.2.1.6, also known as acetolactate synthase) is found, it plays a role in the biosynthesis pathways of the branch-chain amino acids leucine, isoleucine, and valine. AHAS catalyzes the first common step of this pathway. The reactions involve the irreversible decarboxylation of pyruvate and the condensation of the two-carbon fragment with a second molecule of pyruvate, yielding 2-acetolactate, or with a molecule of 2-ketobutyrate, yielding 2-aceto-2-hydroxybutyrate [1,2].

AHAS requires thiamine diphosphate (ThDP) and a divalent metal ion as obligatory cofactors to function. It also requires FAD as a non-catalytic cofactor [1,2]. As the reaction catalyzed by AHAS involves neither oxidation nor reduction, there is no clear explanation as to why the enzyme requires FAD. Recently, Tittmann and co-workers reported that the enzyme-bound FAD in AHAS is reduced as a side reaction in a course of catalysis [3]. Their finding

Abbreviations: AHAS, Acetohydroxy acid synthase; mAHAS, Mutant AHAS; wAHAS, Wild type AHAS; CD, Circular dichroism; FAD, Flavine adenine dinucleotide; GSH, Glutathione; GST, Glutathione *S*-transferase; IPTG, Isopropyl-β-D-thiogalactoside; PCR, Polymerase chain reaction; pGEX–AHAS, Plasmid derived from pGEX-2T containing tobacco AHAS cDNA; ThDP, Thiamine diphosphate; TP, Triazolopyrimidine sulfonamide

* Corresponding author. Fax: +82 43 267 2306.
E-mail address: jdchoi@chungbuk.ac.kr (J.-D. Choi).
[1] Present address: The Microbial Engineering Laboratory, National Food Research Institute, Tsukuba, Ibaraki, Japan.

1570-9639/$ - see front matter © 2005 Elsevier B.V. All rights reserved.
doi:10.1016/j.bbapap.2005.02.012

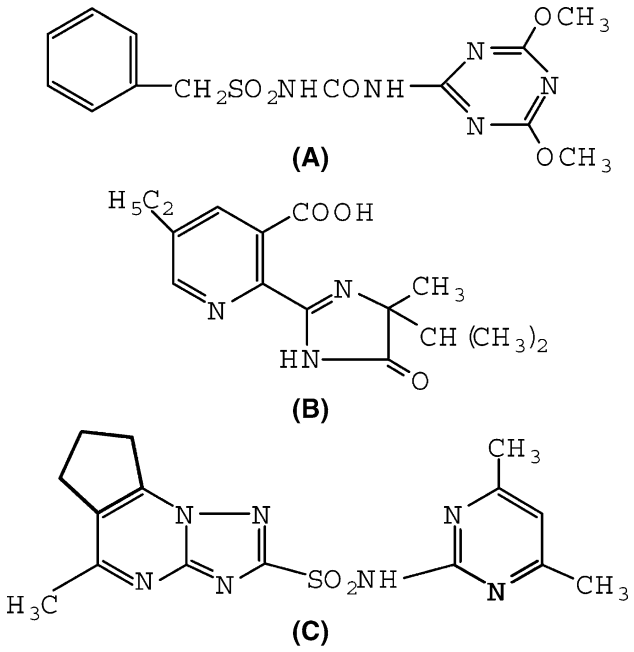

Fig. 1. Structures of AHAS-inhibiting herbicides used in this study. Sulfonylurea Londax (A), Imidazolinone Cadre (B), and Triazolopyrimidine TP (C).

supports the idea of a common ancestor of AHAS and pyruvate oxidase, a homologous ThDP- and FAD-dependent enzyme which, in contrast to AHAS, catalyzes a reaction dependent on intercofactor electron transfer.

AHAS has drawn a great deal of interest recently, as it was identified as the target of several structurally unrelated herbicides [4], including sulfonylureas [4,5], imidazolinones [6], triazolopyrimidines [7,8], and pyrimidyl oxybenzoate [9,10]. The structures of various AHAS-inhibiting herbicides used in this study are shown in Fig. 1. Several of these herbicides are slow and tight-binding inhibitors, which exhibit complex inhibition kinetics [11–13]. Although the AHAS herbicides are potent, their mode of action has yet to be established. It has been suggested that its characteristic inhibition is either uncompetitive or non-competitive [11,14]. Several mutants with resistance to herbicides have been isolated, and, in most cases, this resistance is due to a dominant or semi-dominant mutation in the catalytic subunit gene of AHAS (Summarized in Ref. [2]). Recently, we have reported several herbicide-resistant mutants of tobacco AHAS [15]. However, those herbicide-resistant mutants exhibit relatively low affinity for its pyruvate substrates. As the substrate concentration inside the plant organelles is quite low, mutants with a low affinity for substrate may not function properly in the plant organelles. In this work, we constructed several mutations, with the assistance of the homology model constructed previously, in order to identify an herbicide-resistant mutant, which also exhibits kinetic parameters similar to that of the wild type enzyme.

Bartlett and coworkers studied the functional amino acid residues in structurally known enzymes and found that, among 178 enzymes analyzed, 15% of the functional residues were aspartic acid [16]. Analysis of the protein sequences of 17 AHASs from plants and algae showed that the average number of aspartic acid residues was approximately 33. Among these, 9 residues are identical in 17 sequences (Fig. 2). Multiple sequence analysis revealed two aspartic acid residues located consecutively in the β-domain of tobacco AHAS. The two residues are located in a highly conserved motif ($_{372}$RFDDR$_{376}$). In the recently-constructed structure model of tobacco AHAS [17] based on yeast X-ray

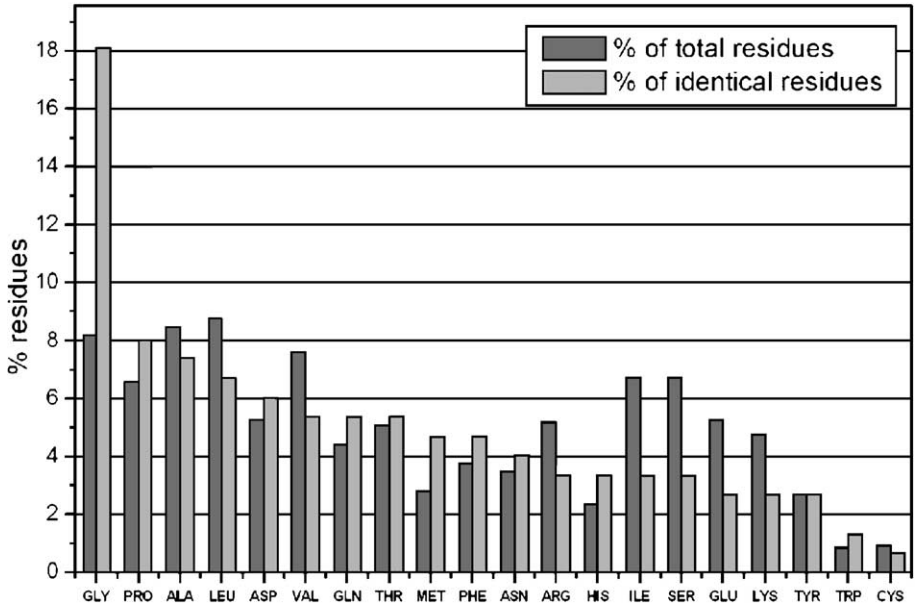

Fig. 2. Distribution of amino acid types and their conservation in 17 AHAS protein sequences from plants and algae. The sequences analyzed included the transit peptide signals. Aspartic acid is among the most functional conserved group, comprising an average of 9 conserved residues among 33 total aspartic acid residues.

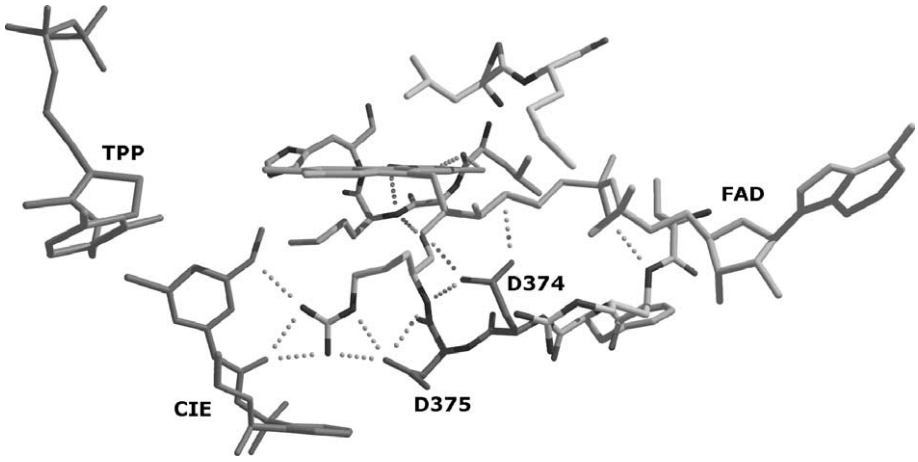

Fig. 3. Structural model of tobacco AHAS constructed based on the yeast AHAS template (1N0H.pdb) showing the involvement of the two residues in this study in the herbicide-binding and FAD-binding sites. CIE is a sulfonylurea chlorimuron ethyl; dotted lines represent hydrogen bonds. R376 interacts directly with CIE. This figure was generated using Molecular Image (Molw 4.0) and Showcase software.

structure [18] the two residues are located close to the herbicide sulfonylurea and the cofactor FAD (Fig. 3). In addition to that, Duggleby et al. recently reported the systematic characterization of herbicide-resistant mutations in yeast AHAS [19]. In their report, the D379N mutant of yeast AHAS, which is equivalent to the D375 residue in tobacco AHAS, was strongly resistant to sulfonylureas. However, this mutant exhibited a high degree of sensitivity to imidazolinone [19].

In order to design herbicide-resistant mutants of this enzyme, we performed site-directed mutagenesis on these two aspartic acid residues. The mutants obtained were evaluated for herbicide sensitivity against a sulfonylurea Londax, an imidazolinone Cadre, and a triazolopyrimidine TP. The kinetic and structural properties of these mutants were also determined, and the data obtained will be discussed in relation to the homology model.

2. Materials and methods

2.1. Materials

LB Broth (Luria-Bertani) and LB Agar were purchased from Difco Laboratories (Detroit, USA). Restriction enzymes were purchased from Roche Co. (Mannheim, Germany). GSH, Sephadex G-25, ThDP, FAD, α-naphthol, and creatine were obtained from Sigma Chemical Co. (St. Louis, USA). Thrombin protease and epoxy-activated Sepharose 6 B were obtained from Pharmacia Biotech (Uppsala, Sweden). *E. coli* XL1-Blue cells containing the expression vector pGEX-AHAS were provided by Dr. Soo-Ik Chang (Chungbuk National University, Cheongju, Korea). Oligonucleotides were obtained from Genotech (Daejon, Korea). Londax (a sulfonylurea herbicide) and Cadre (an imidazolinone herbicide) were provided by Dr. Dae-Whang Kim (Korea Research Institute of Chemical Technology, Daejon, Korea). TP, a triazolopyrimidine derivative, was obtained from Dr. Sung-Keon Namgoong (Seoul Women's University, Seoul, Korea).

2.2. Multiple sequence alignment of AHAS sequences

The multiple sequence alignment was carried out using ClustalW [20] with the 17 AHAS sequences described previously as a data set [21]. This sequence data set was also used to calculate the conserved residues (as shown in Fig. 2). The sequences used for the calculation included the transit signal peptides.

2.3. Site-directed mutagenesis

Site-directed mutagenesis of tobacco AHAS was performed directly on the plasmid derived from pGEX-2T containing tobacco AHAS cDNA, using the PCR mega-primer method [22]. All manipulations of the DNA were carried out using the techniques reported previously [23]. The initial PCR was performed with oligonucleotide primer NKB2 and each mutagenic fragment as internal primers with the low-cased bases changed as follows:

NKB2, 5′-CCCG**GGATCC**TCAAAGTCAATA-3′
D374A, 5′-GGTGAGGTTT*GcT*GATAGAGTTAC-3′
D374E, 5′-GGTGAGGTTT*GAa*GATAGAGTTAC-3′
D375A, 5′-GAGGTTTGAT*GcT*AGAGTTACTGG-3′
D375E, 5′-GAGGTTTGAT*GAa*AGAGTTACTGG-3′
D34A/D375A, 5′-GGTGAGGTTT*GcTGcT*AGAGTTAC-3′
D374E/D375E, 5′-GGTGAGGTTT*GAaGAa*AGAGTTAC-3′

The bold bases in the NKB2 primer represent BamHI restriction sites. The resultant DNA was subjected to a second PCR with the universal primer NKB1 5′-CATCTCCGGATCCATGTCCACTACCCAA-3′. The PCR products were double-digested with NcoI and BglII, and

cloned into the expression vector, which was prepared from the NcoI/BglII-excised pGEX–wAHAS. The resultant pGEX–mAHAS was used to transform the *E. coli* strain XL1-Blue cells, using standard $CaCl_2$ transformation protocols [23]. Each transformant was identified by the digestion of its plasmid with BamHI, with subsequent sequencing to ensure correct base mutations.

2.4. DNA sequence analysis

DNA sequencing was carried out via the dideoxy chain-termination procedure [24] at Macrogen, Inc. (Seoul, Korea).

2.5. Expression and purification of tobacco wAHAS and mAHAS

Bacterial strains of *E. coli* BL21-DE3 cells, containing the expression vector pGEX–AHAS, were grown at 37 °C in Luria–Bertani (LB) broth medium containing 50 μg/ml ampicillin, to an OD_{600} of 0.7–0.8. Expression of the pGEX-AHAS gene was induced by the addition of 0.1–0.3 mM isopropyl-D-thiogalactoside (IPTG). Cells were grown for an additional 4 h at 30 °C, then harvested by centrifugation at 5000 g for 30 min. Purification of wAHAS and mAHAS was performed as described previously by Chang et al. [25]. The cell pellets were suspended in standard buffer (50 mM Tris–HCl, pH7.5, 1 mM pyruvate, 10% (v/v) ethylene glycol, 10 mM $MgCl_2$) containing protease inhibitors. The cell suspension was then lysed by sonication at 4 °C. The homogenate was centrifuged at 20,000 ×*g* for 20 min twice, and the supernatant was applied to the GSH-coupled Sepharose 6 B column, at which the unbound proteins were removed by washing with standard buffer. The GST–AHAS fusion protein was recovered from the column with an elution buffer (50 mM Tris–HCl, pH7.5, 15 mM GSH, and 10% (v/v) ethylene glycol). In order to obtain the cleaved AHAS, the purified GST–AHAS was incubated overnight at 4 °C with thrombin (10 U/mg protein). The AHAS was purified by an additional GSH-affinity chromatography step. The isolated protein was identified via SDS-PAGE analysis [26], and the protein concentration was determined by the method of Bradford [27].

2.6. Enzyme assay

The enzyme activities of the purified wAHAS and mAHAS were measured according to the method of Westerfeld [28], with slight modification, as reported previously [29]. The reaction mixture contained a 50 mM potassium phosphate buffer (pH7.5), 1 mM ThDP, 10 mM $MgCl_2$, 20 μM FAD, 100 mM pyruvate, and the enzyme, in the absence or presence of different concentrations of cofactors or inhibitors. The reaction starts by adding the enzyme solution into the buffer containing substrate and cofactors at 37 °C and ends by the addition of 6 N H_2SO_4. Unless otherwise specified, the values of V_{max}, and K_m for the substrate were determined by fitting the data into Eq. (1), while the activation constant (K_a) values were obtained by fitting the data into Eq. (2).

$$v = V_{max}/(1 + K_m/[S]) \quad (1)$$

$$v = V_0 + V_{max}/(1 + K_a/[C]) \quad (2)$$

In these equations, v is the reaction velocity, V_{max} is the maximum velocity, V_0 is the activity due to the trace of cofactors present in the apo-enzyme, K_m is the Michaelis Menten constant, K_a is the activation constant, $[S]$ is the substrate concentration, and $[C]$ is the concentration of added cofactor. The K_i^{app} values were determined by fitting the data into Eq. (3).

$$v_i = v_0/\left(1 + [I]/K_i^{app}\right) \quad (3)$$

In this equation, v_i and v_0 represent the rate in the presence or absence of the inhibitor, respectively, and $[I]$ is the concentration of the inhibitor. The K_i^{app} is the apparent K_i, that is, the concentration of the inhibitor resulting in 50% inhibition under standard assay conditions. This is also known as the IC_{50}. All fittings and data analysis were conducted using the Sigma Plot 8.0 program (Systat Software Inc., California, USA).

2.7. Spectroscopic studies

Absorption spectra were recorded on a Beckman DU-600 Spectrophotometer. The protein solution was dispensed in 1 ml black-walled quartz cuvettes, and the spectrum of each sample was scanned over a range of 250–550 nm. Fluorescence emission spectra were recorded with a Hitachi F-3000 fluorescence spectrophotometer. The fluorescence emission spectra of FAD bound to wAHAS and mAHAS were scanned over a range of 450–650 nm, via excitation at 370 nm. The bandwidth for excitation and emission was 5 nm. The far-UV CD spectra were recorded over a range of 190–250 nm on a Jasco J-710 Spectropolarimeter set at 50 mdeg sensitivity, 1 mm resolution, 3 units accumulation, 5 s response, and at a scanning speed of 200 nm/min. A protein solution of 0.36 mg/ml was assayed in a cylindrical quartz cell with a path length of 1 mm. Near-UV CD spectra were determined using a protein solution of 0.2 mg/ml in a cylindrical quartz cell with a 20-mm path length, on the same machine. The near-UV CD spectra were recorded in a wavelength region of 240–340 nm.

2.8. Analysis of structural models

The structure of the homology model [17] was analyzed by Deep View [30,31] and Molw 4.0. Structural illustrations were created from coordinate files with Deep View

Table 1
Kinetic parameters of the wild type and mutant AHASs

Enzymes	V_{max} (U mg^{-1})	K_m (pyruvate, mM)	V_{max}/K_m	Affinity for FAD			Affinity for ThDP		
				V_0	K_{FAD}[a] (μM)	Activation efficiency[a]	V_0	K_{ThDP}[a] (μM)	Activation efficiency
wAHAS	1.55 ± 0.05	11.7 ± 1.9	132.5×10^{-3}	0.96	20.9 ± 3.5	28.5×10^{-3}	0.86	28.2 ± 3.8	23.6×10^{-3}
D374A[b]	0.91 ± 0.15	5.7 ± 2.4	159.7×10^{-3}	0.51	34.5 ± 4.3	11.6×10^{-3}	0.23	2.5 ± 0.3	266.7×10^{-3}
D374E	0.77 ± 0.10	557.6 ± 141.1	1.4×10^{-3}	0.03	168.6 ± 15.8	4.4×10^{-3}	0.00	774.2 ± 244.5	0.97×10^{-3}
D375A	0.65 ± 0.07	109.3 ± 37.2	5.9×10^{-3}	0.07	9.1 ± 0.3	64.4×10^{-3}	0.02	134.8 ± 57.8	4.7×10^{-3}
D375E	1.53 ± 0.06	3.6 ± 0.8	425.0×10^{-3}	1.2	3.1 ± 0.5	103.1×10^{-3}	1.35	6.6 ± 0.6	27.3×10^{-3}
D374A/D375A	0.09 ± 0.00	55.8 ± 5.9	1.6×10^{-3}	0.02	5.9 ± 0.5	11.9×10^{-3}	0.01	93.1 ± 16.6	0.86×10^{-3}
D374E/D375E	0.64 ± 0.05	266.7 ± 42.4	2.4×10^{-3}	0.03	46.5 ± 7.8	13.2×10^{-3}	0.00	76.2 ± 4.7	8.4×10^{-3}

[a] Activation efficiency was calculated using following equation: $(V_{max} - V_0)/K_a$.
[b] The D374A mutant was inhibited by high substrate concentrations; its V_{max}, K_m and K_i (substrate inhibition constant) were determined by fitting of data to empirical equation, $v = V_{max}[Pyr]/(K_m + [Pyr](1 + [Pyr]/K_i))$, given the K_i/K_m ratio of 34.6.

and Molw PDB Viewer 4.0 with Showcase (http://www.molimage.com).

3. Results

3.1. Asp374 mutants

In order to reveal the roles of this residue in the proposed herbicide-binding site (Fig. 3), two different mutations were individually performed on this residue, resulting in two active mutants (D374A and D374E). While the two mutants exhibited insignificant changes in their V_{max} values, their affinities for pyruvate proved to be distinct. As shown in Table 1, the K_m value of the D374A mutant was half that of the wild type. However, this value in the D374E mutant was almost 48-fold higher than the corresponding wild-type value. The activation efficiencies by FAD of the D374A and D374E mutants were 11.6×10^{-3} and 4.4×10^{-3}, respectively. The corresponding value for wAHAS was 28.5×10^{-3}. The activation efficiency of the D374A mutant by ThDP was 11-fold higher than that of the wild type. However, this value in the D374E mutant was 24-fold lower than that of the wild type (Table 1). Surprisingly, while the phenomenon of substrate inhibition was not observed with wAHAS, the D374A mutant was strongly inhibited at high substrate concentrations, given a K_i/K_m ratio of 34.6 (Fig. 4). The D374A mutant was strongly cross-resistant to Londax and Cadre, while the D374E mutant was strongly resistant to Londax, but not Cadre (Table 2 and Fig. 8). The absorption and fluorescence spectra of FAD bound to the two mutant enzymes were determined. Fig. 5 shows that, while the D374A mutant harbors a significant amount of bound FAD, only a small amount of enzyme-bound FAD was detected in the D374E mutant, using the same technique. The far-UV CD spectra of these two mutant

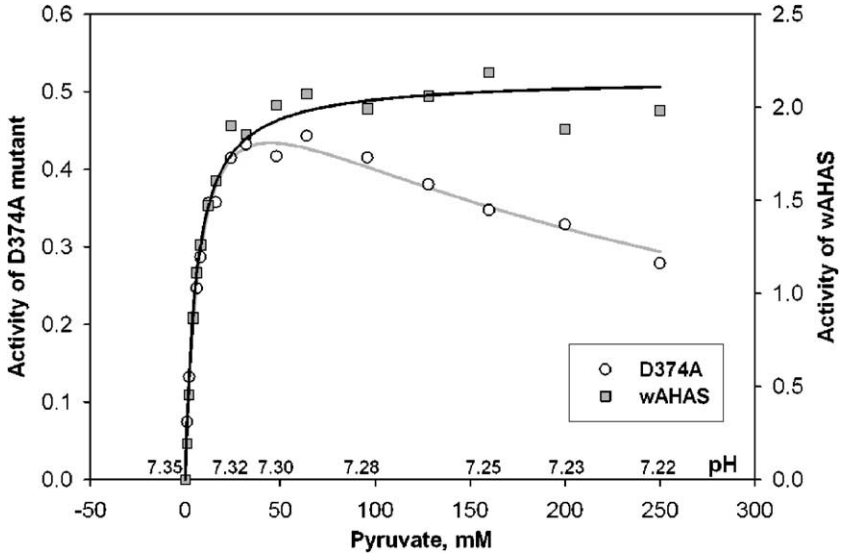

Fig. 4. The pyruvate-dependent activity of wAHAS and D374A mutant, substrate inhibition was observed with D374A mutant. The values of V_{max}, K_m, K_i of the D374A mutant were obtained by fitting data into the empirical equation $v = V_{max}[Pyr]/(K_m + [Pyr](1 + [Pyr]/K_i))$. The ratio of K_i/K_m (34.6) of this mutant indicates that the inhibition by substrate is quite robust. The values at the upper part of the X-axis indicate the pH values of the assay solutions at corresponding pyruvate concentrations.

Table 2
K_i^{app} values for three classes of herbicides of the wild type and mutant AHASs

Enzymes	Londax (nM)	Cadre (μM)	TP (μM)
wAHAS	13.0 ± 0.8	4.1 ± 0.5	29.3 ± 2.9
D374A	860 ± 110.5	181 ± 15.7	74.1 ± 3.8
D374E	108.4 ± 1.3	15.5 ± 1.9	36 ± 3.3
D375A	N.D (>1 μM)	0.8 ± 0.2	198.5 ± 30.4
D375E	N.D (>1 μM)	38.9 ± 2.4	N.D (>1mM)
D374A/D375A	N.D (>1 μM)	13.3 ± 4.4	309.2 ± 27.6
D374E/D375E	N.D (>5 μM)	29.6 ± 3.1	790.2 ± 89.2

The K_i^{app} values were obtained by fitting of the observed data into the equation $v_i = v_0/(1+[I]/K_i^{app})$ using Sigma Plot program (Systat Software Inc., California, USA,), N.D., not detectable experimentally, the values in parentheses are the predicted values by further extrapolation of the experimental data.

enzymes were similar to that of wAHAS. That notwithstanding, both mutants exhibited near-UV CD spectra which were significantly different from that of the wild type enzyme. The peaks of the near-UV CD spectra of both mutants were shifted to longer wavelengths, suggesting a possible change occurring in the overall structural conformation of the two mutants (Fig. 6).

3.2. Asp375 mutants

In order to determine the functions of this residue, we carried out two single-point substitutions and obtained two active mutants, designated D375A and D375E. The V_{max} values of the two mutants were 0.65 and 1.53, respectively. While the K_m value of the D375A mutant was 10-fold higher than that of the wild type enzyme, this value in the D375E mutant was 3-fold lower (Table 1). FAD bound to these two mutants was easily visualized by its fluorescence emission after specific excitation. Furthermore, the fluorescence intensity of the spectrum of the D375E mutant was almost twice of that of the wild type (Fig. 5, inset). While the activation efficiency of the wild type by FAD was 28.5×10^{-3}, these values in the D375A and D375E mutants were 64.4×10^{-3} and 103.1×10^{-3}, respectively. The activation efficiency of the D375A mutant by ThDP was 5-fold less than that exhibited by the wild type enzyme. This value in the D375E mutant was similar to that of wAHAS (Table 1). The two mutants were also evaluated for their sensitivity to the herbicides Londax, Cadre, and TP. The two mutants were strongly cross-resistant to Londax and TP, but not to Cadre. Interestingly, the D375A mutant was 5-fold more sensitive to Cadre as compared to the wild type (Table 2 and Fig. 8). In order to determine whether the mutations induced any structural alterations in the enzyme, the CD spectra of the wild type and mutants were recorded in the far-and near-UV regions. According to our data, however, the far- and near-UV CD spectra of the mutants were similar to that of the wild type enzyme (Fig. 6 and data not shown).

3.3. Double mutants of Asp374 and Asp375

As the two residues are located consecutively, effects due to the removal of the side chain of either of the two residues may be counterbalanced by the side chain of the other. In order to characterize the functions of these two presumably negatively charged residues in more detail, we carried out two double mutations, resulting in two active mutants, D374A/D375A and D374E/D375E (Table 1). The V_{max} values of these two mutants were 0.09 and 0.64, respectively. The catalytic efficiencies of the two mutants also

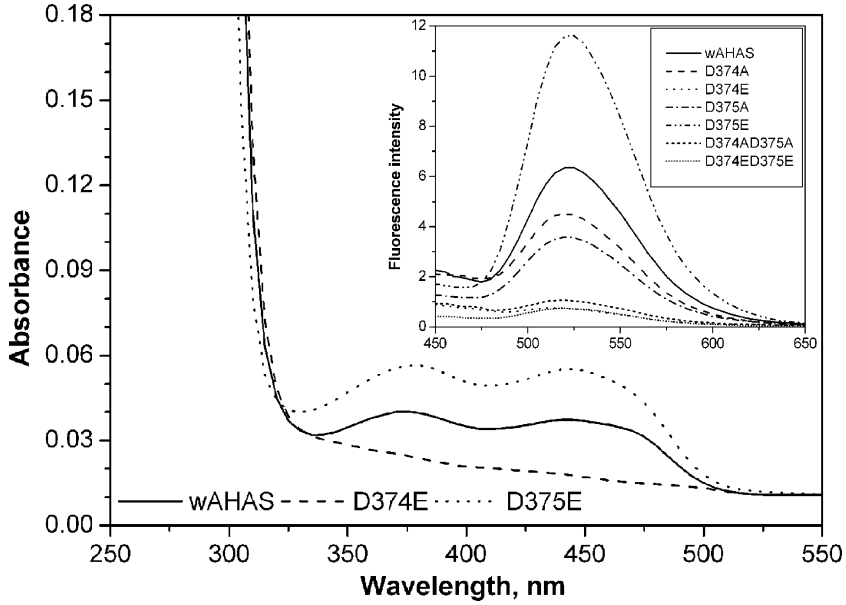

Fig. 5. Absorbance and fluorescence (inset) spectra of both wild type and mutant enzymes. Data indicated that the D375E mutant contains a higher level of bound-FAD, and that the two double mutants and D374E mutants did not contain a significant amount of bound-FAD.

substantially decreased (Table 1). The FAD bound to the two mutants could only barely be detected by observations of the absorbance and fluorescence spectra (Fig. 5), and the activation efficiencies of the two mutants by FAD were also found to be attenuated to less than half of the value of the wild type enzyme (Table 1). The activation efficiency of the D374A/D375A mutant by ThDP was 27-fold lower than that of the wild type enzyme, while this value in the D374E/D375E mutant was just 2.8-fold lower (Table 1). This suggests that there was a synergistic reduction in the V_{max} value and the binding affinity to FAD of the D374A/D375A mutant, as the V_{max} values of each of the single-point mutations D374A and D375A were roughly 10-fold higher than that of the double mutants, and the FAD bound to each of the single-point mutations D374A and D375A was also detectable by fluorescence spectra. Nevertheless, the FAD bound to the double mutant was only barely detectable by the same technique. The far-UV CD spectra of the double mutants were similar to that of the wild type, however, only the near-UV CD spectrum of the D374A/D375A mutant remained similar to that of the wild type enzyme (Fig. 7).

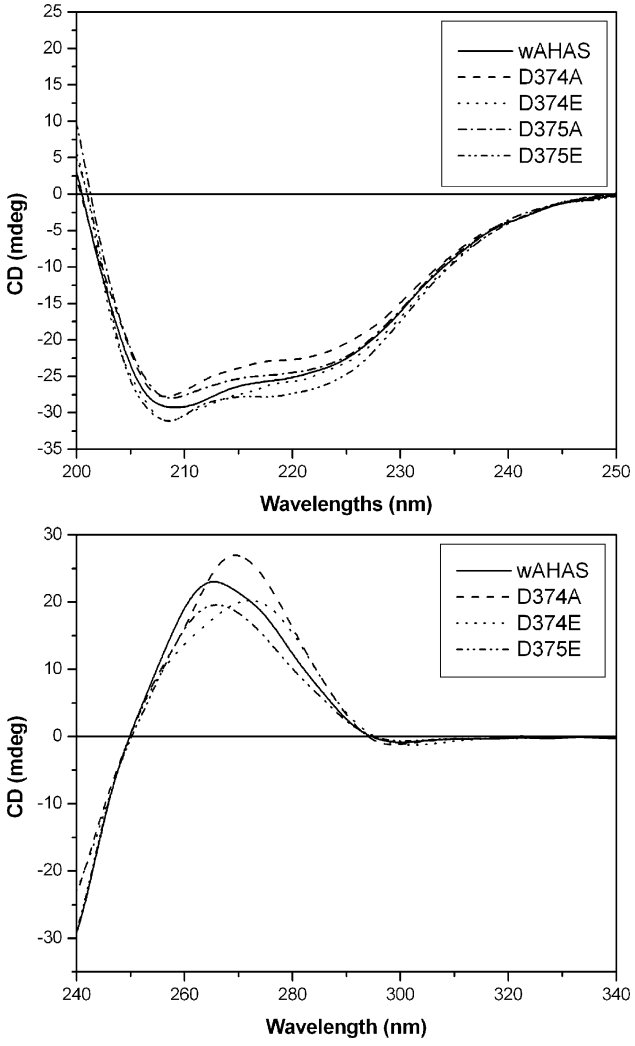

Fig. 6. Far- and near-UV CD spectra of the wild type and single-substitution mutant enzymes. Samples for far-UV CD assays contain 0.36 mg/ml protein, while samples for near-UV CD measurement contain 0.2 mg/ml protein.

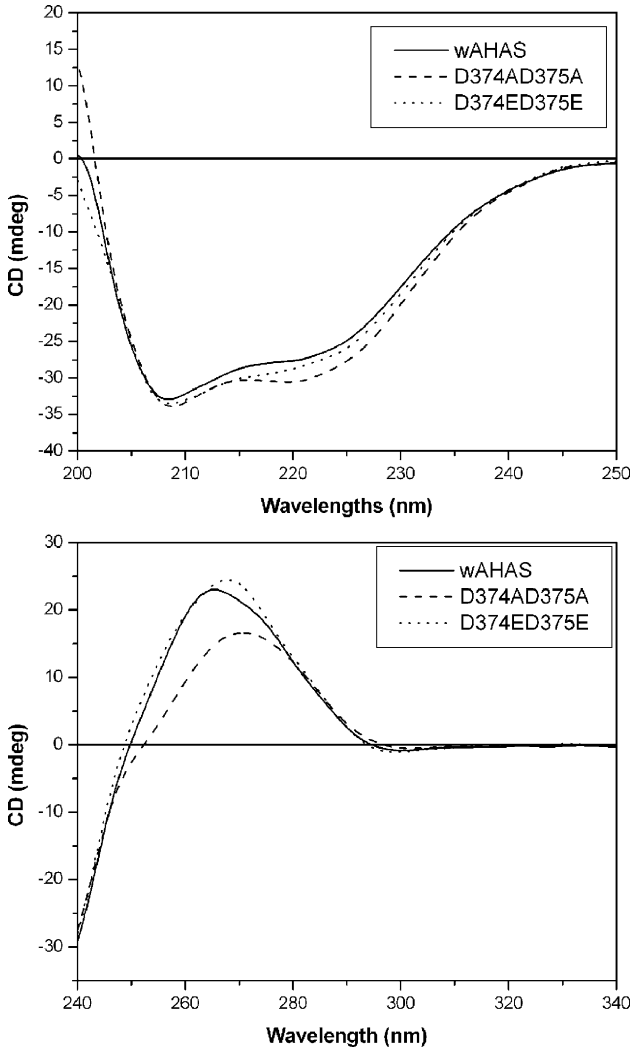

Fig. 7. CD spectra of the wild type and double mutant enzymes in the far- and near-UV regions. Samples for far-UV CD assays contain 0.36 mg/ml protein, while the samples for near-UV CD measurement contain 0.2 mg/ml protein.

4. Discussion

In an attempt to determine the distribution frequency of each amino acid involved in the catalysis, Bartlett and coworkers previously performed a comprehensive study of functional amino acid residues in enzymes with known structures [16]. Their study revealed that, among the catalytic residues of the 178 enzymes analyzed, 15% were aspartic acid, comprising the second most abundant residue [16]. In order to ascertain this distribution in AHAS, we analyzed the protein sequences of 17 AHASs from plants and algae. Our data revealed that, in 17 AHAS sequences, the average number of aspartic acid residues is about 33. Among these residues, 9 are identical (Fig. 2). Taking into consideration

the multiple sequence alignment of the 17 AHASs from plants and algae, we identified 2 highly conserved and consecutively-located aspartic acid residues. With regard to the homology model, these two residues are likely located within a highly conserved motif ($_{372}$RFDDR$_{376}$), and were positioned very proximally to the FAD cofactor (Fig. 3). The model also suggests that sulfonylurea herbicide binds to the enzyme at this site. In fact, the herbicide chlorimuron ethyl interacts directly with the R376 residue, and the R376 residue is supported by two hydrogen bonds from the D375 residue. Furthermore, the equivalent residue of tobacco AHAS R376 in *E. coli* AHAS was implicated in condensation with the second keto acid [32]. Thus, we assumed that the positively charged group of residue R376 might be important for the catalytic function. Hence, instead of mutating this residue, we prefer to alter the nearby environment, namely residues D374 and D375. We predicted that these two residues might also prove important, with regard to both catalytic activity and herbicide sensitivity. To study the function of the selected residues, we first mutated to alanine to reveal the importance of the negatively charged groups, and then we increased the size of the negatively charged group, by mutating it to glutamic acid, to see how the bigger negatively charged group function at this particular position.

We constructed four single-point mutations (D374A, D374E, D375A and D375E) and two double mutations (D374A/D375A and D374E/D375E). All the single-point mutations had only insignificant effects on the V_{max} of the enzyme (Table 1). The two mutants D374A and D375E exhibit lower K_m values than that of the wild type. Furthermore, the D374A mutant is inhibited at high substrate concentrations. This pyruvate substrate-induced inhibition is quite robust, with a K_i/K_m ratio of 34.6 (Fig. 4). This indicates that the mutation to alanine at residue D374 may have altered the herbicide-binding site in such a way that it allows an additional pyruvate substrate to bind, and then function as an inhibitor. As the D374 residue contributes several hydrogen bonds to other residues within the RFDDR motif (Fig. 3), the alanine substitution may also affect the conformation of the motif which causes the formation of the new binding site for pyruvate. Although substrate inhibition was not observed in wild type tobacco AHAS, it does present in bacterial AHAS [33]. Porat and coworkers recently cloned a thermostable AHAS from *B. stearothermophilus* and expressed it in *E. coli.* They determined that this enzyme exhibited substrate inhibition activity [33].

Among our four single-point mutants, the D374 mutants exhibited the least affinity for FAD (Table 1). However, the activation efficiencies of the D375 mutants by FAD are higher than that of the wild type. As the activation efficiency of the D375E mutant by ThDP is similar to that of wAHAS, it would appear that this mutation has no effect on binding and activation by ThDP. On the other hand, this mutant has a K_m value for pyruvate which is 3-fold lower than that of the wild type enzyme. The activation efficiency of the D374A mutant by ThDP is 11-fold higher than that of the wild type enzyme, indicating that the mutation may favor binding and activation by ThDP.

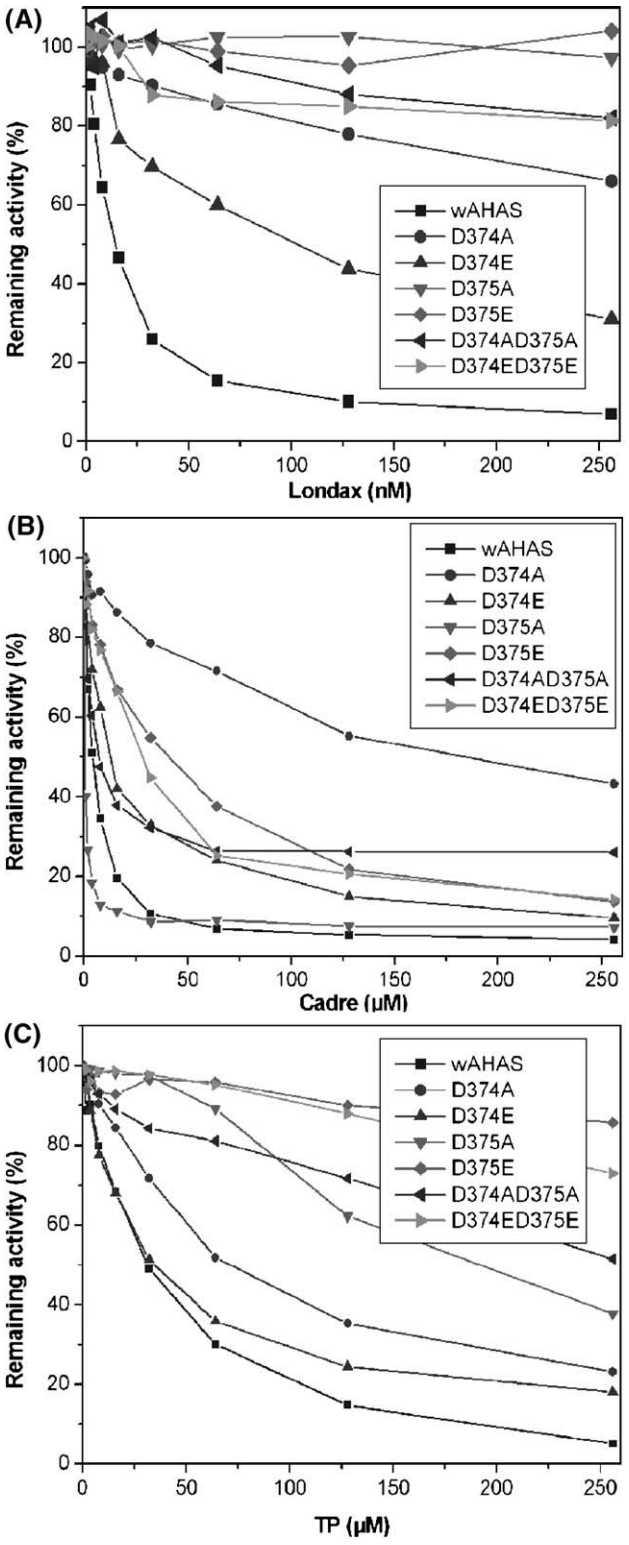

Fig. 8. Remaining activity of the wild type and mutant enzymes as a function of herbicide concentration. A, sulfonylurea Londax; B, imidazolinone Cadre; C, triazolopyrimidine TP.

All mutants in this study proved to be strongly resistant to Londax. The double mutants and mutants of D375 were also strongly cross-resistant to TP. Among all the constructed mutants, only the D374A mutant exhibited robust cross-tolerance to Cadre (Table 2 and Fig. 8). In recent report by Duggleby's group, the D379N mutant of yeast AHAS, which is equivalent to the D375 residue in tobacco AHAS, was resistant only to sulfonylureas. Furthermore, this mutant exhibited a high degree of sensitivity to imidazolinone [19]. Our work with plant AHAS was somewhat consistent with their report, as we discovered that the D375A mutant was 5-fold more sensitive to imidazolinone Cadre than the wild type. Additionally, both D375A and D375E mutants proved strongly resistant to sulfonylurea Londax (Table 2 and Fig. 8). We also showed here that both mutants exhibited moderate-to-high levels of resistance to triazolopyrimidine TP (Table 2 and Fig. 8). With regard to kinetic parameters and herbicide insensitivity, the D375E mutation provides a valuable mutant construct for the development of herbicide resistant transgenic plants.

In order to gain further understanding of the function of these two negatively charged residues in terms of their interaction with herbicides, we conducted an alanine replacement in both residues, which resulted in the D374A/D375A mutant. This mutant is active, we observed a synergistic reduction in its V_{max} value, as compared to the values associated with the single-point mutants and wAHAS. Our data, therefore, indicate that the presence of these negatively charged groups at this particular position is important, but not absolutely required, for the activity of the enzyme. It should be noted that the substrate inhibition phenomenon in the D374A mutant was not observed in the double mutant D374A/D375A. It is now clearer that the formation of a new binding site for pyruvate is not solely due to the removal of the negatively charged group at residue D374, but also to the new conformation of the RFDDR motif resulting from the mutation. An additional mutation of D375A in the D374A mutant (formed D374A/D375A mutant) resulted in the elimination of the new binding site, and hence, substrate inhibition did not occur. Affinity for FAD and ThDP was also reduced in the D374A/D375A mutant.

In conclusion, the two residues, D374 and D375, are located at a common binding site for the sulfonylurea and triazolopyrimidine herbicides, and this may overlap to some degree with the regions in which the cofactor binding sites for FAD and ThDP are located. The D375E mutant appears to be a good candidate for the development of herbicide-resistant transgenic plants.

Acknowledgments

We thank Dr. Dae-Whang Kim (Korea Research Institute of Chemical Technology, Korea) for providing us with Londax and Cadre, and Dr Sung-Keon Namgoong (Seoul Women's University, Korea) for providing us with TP. This work was supported by Korea Research Foundation Grant KRF-2002-070-C0064.

References

[1] N. Gollop, B. Damri, Z. Barak, D.M. Chipman, Kinetics and mechanism of acetohydroxy acid synthase isozyme III from *Escherichia coli*, Biochemistry 28 (1989) 6310–6317.
[2] R.G. Duggleby, S.S. Pang, Acetohydroxyacid synthase, J. Biochem. Mol. Biol. 33 (2000) 1–36.
[3] K. Tittmann, K. Schröder, R. Golbik, J. McCourt, A. Kaplun, R.G. Duggleby, Z. Barak, D. Chipman, G. Hübner, Electron transfer in acetohydroxy acid synthase as a side reaction of catalysis: implications for the reactivity and partitioning of the carbanion/enamine form of (-hydroxyethyl) thiamin diphosphate in a "nonredox" flavoenzyme, Biochemistry 43 (2004) 8652–8661.
[4] R.A. LaRossa, J.V. Schloss, The sulfonylurea herbicide Sulfometuron is an extremely potent and selective inhibitor of acetolactate synthase in *Salmonella typhimurium*, J. Biol. Chem. 259 (1984) 8753–8757.
[5] J.B. Ray, Site of action of chlorosulfuron: inhibition of valine and isoleucine biosynthesis of plants, Plant Physiol. 75 (1984) 827–831.
[6] D.L. Shaner, P.C. Anderson, M.A. Stidham, Imidazolinones: potent inhibitors of acetohydroxy acid synthase, Plant Physiol. 76 (1984) 545–546.
[7] W.A. Kleschick, M.J. Costales, J.E. Dunbar, R.W. Meikle, W.T. Monte, N.R. Pearson, S.W. Snider, A.P. Vinogradoff, New herbicidal derivatives of 1,2,4-triazolo[1,5-a]pyrimidine, Pestic. Sci. 29 (1990) 341–355.
[8] B.C. Gerwick, M.V. Subramanian, V. Loney-Gallant, D.P. Chander, Mechanism of action of the 1,2,4-triazolo [1,5,a-] pyrimidine, Pestic. Sci. 29 (1990) 357–364.
[9] P. Babczinski, T. Zelinski, Mode of action of herbicidal ALS-inhibitors on acetolactate synthase from green plant cell cultures, yeast, and *Escherichia coli*, Pestic. Sci. 31 (1991) 305–323.
[10] J.-D. Choi, H. Moon, S.-I. Chang, J.-K. Chae, J.-H. Shin, Inhibition of acetolactate synthase by prpyrimidyl-oxy-benzoate and pyrimidyl-thio-benzenes, J. Biochem. Mol. Biol. 26 (1993) 638–643.
[11] J.V. Schloss, Interaction of the herbicide sulfometuron methyl with acetolactate synthase: a slow-binding inhibitor, in: R.C. Bray, P.C. Engel, S.G. Mayhew (Eds.), Flavins and Flavoproteins, Walter de Gruyter, Berlin, 1984, pp. 737–740.
[12] B.K. Singh, D.L. Shaner, Biosynthesis of branched-chain amino acids: from test tube to field, Plant Cell 7 (1995) 935–944.
[13] J.V. Schloss, Recent advances in understanding the mechanism and inhibition of acetolactate synthase, in: J. Stetter (Ed.), Herbicides Inhibiting Branched Chain Amino Acid Biosynthesis, Springer-Verlag, Germany, 1994, pp. 4–14.
[14] G.M. Kishor, D.M. Shah, Amino acid biosynthesis inhibitors as herbicides, Annu. Rev. Biochem. 57 (1988) 627–663.
[15] S.-M. Jung, D.T. Le, S.-S. Yoon, M.-Y. Yoon, Y.T. Kim, J.-D. Choi, Amino acid residues conferring herbicide-resistance in tobacco acetohydroxy acid synthase, Biochem. J. 383 (1) (2004) 53–61.
[16] G.J. Bartlett, C.T. Porter, N. Borkakoti, J.M. Thornton, Analysis of catalytic residues in enzyme active sites, J. Mol. Biol. 324 (2002) 105–121.
[17] D.T. Le, M.-Y. Yoon, Y.T. Kim, J.-D. Choi, Homology modeling and examination of the active site of tobacco acetohydroxy acid synthase, Biochem. Biophys. Res. Commun. 317 (3) (2004) 930–938.
[18] S.S. Pang, L.W. Guddat, R.G. Duggleby, Molecular basis of sulfonylureas herbicide inhibition of acetohydroxy acid synthase, J. Biol. Chem. 278 (2003) 7639–7644.
[19] R.G. Duggleby, S.S. Pang, H. Yu, L.W. Guddat, Systematic characterization of mutations in yeast acetohydroxy acid synthase:

interpretation of herbicide-resistance data, Eur. J. Biochem. 270 (2003) 2895–2904.
[20] J.D. Thompson, D.G. Higgins, T.J. Gibson, CLUSTALW: improving the sensitivity of progressive multiple sequence alignment through sequence weighting, positions-specific gap penalties and weight matrix choice, Nucleic Acids Res. 22 (1994) 4673–4680.
[21] D.T. Le, M.-Y. Yoon, Y.T. Kim, J.-D. Choi, Roles of conserved methionine residues in tobacco acetolactate synthase, Biochem. Biophys. Res. Commun. 306 (4) (2003) 1075–1082.
[22] G. Sarkar, S.S. Sommer, "Megaprimer" method of site-directed mutagenesis, Biotechniques 2 (1990) 404–407.
[23] J. Sambrook, E.F. Fritsch, T. Maniatis, Molecular Cloning: A Laboratory Manual, 2nd ed., Cold Spring Harbor Laboratory Press, Cold Spring Harbor, New York, USA, 1989.
[24] F. Sanger, S. Nicklen, A.R. Coulson, DNA sequencing with chain-terminating inhibitors, Proc. Natl. Acad. Sci. U. S. A. 74 (1977) 5463–5467.
[25] S.-I. Chang, M.-K. Kang, J.-D. Choi, S.K. Namgoong, Soluble overexpression in *Escherichia coli*, and purification and characterization of wild-type recombinant tobacco acetolactate synthase, Biochem. Biophys. Res. Commun. 234 (1997) 549–553.
[26] U.K. Laemmli, Cleavage of structural proteins during the assembly of the head of bacteriophage T4, Nature 227 (1970) 680–685.
[27] M.M. Bradford, A rapid and sensitive method for the quantification of microgram quantities of protein utilizing the principle of protein-dye binding, Anal. Biochem. 72 (1976) 248–254.
[28] W.W. Westerfeld, A colorimetric determination of blood acetoin, J. Biol. Chem. 161 (1945) 495–502.
[29] C.-K. Chong, S.-I. Chang, J.-D. Choi, Functional amino acid residues of recombinant tobacco acetolactate synthase, J. Biochem. Mol. Biol. 30 (1997) 274–279.
[30] N. Guex, M.C. Peitsch, SWISS-MODEL and the Swiss-PdbViewer: an environment for comparative protein modelling, Electrophoresis 18 (1997) 2714–2723.
[31] T. Schwede, J. Kopp, N. Guex, M.C. Peitsch, SWISS-MODEL: an automated protein homology-modeling server, Nucleic Acids Res. 31 (2003) 3381–3385.
[32] S. Engel, M. Vyazmensky, M. Vinogradov, D. Berkovich, A. Bar-Ilan, U. Qimron, Y. Rosiansky, Z. Barak, D.M. Chipman, Role of a conserved arginine in the mechanism of acetohydroxy acid synthase: catalysis of condensation with a specific ketoacid substrate, J. Biol. Chem. 279 (2004) 24803–24812.
[33] I. Porat, M. Vinogradov, M. Vyazmensky, C.-D. Lu, D.M. Chipman, A.T. Abdelal, Z. Barak, Cloning and characterization of acetohydroxy acid synthase from *Bacillus stearothermophilus*, J. Bacteriol. 186 (2004) 570–574.